ORIGINAL

Identification and functional analysis of a splice variant of mouse sodium-dependent phosphate transporter Npt2c

Shoji Kuwahara[1][*], Fumito Aranami[1][*], Hiroko Segawa[1], Akemi Onitsuka[1],

Naoko Honda[1], Rieko Tominaga[1], Etsuyo Hanabusa[1], Ichiro Kaneko[1],

Setsuko Yamanaka[1], Shohei Sasaki[1], Akiko Ohi[1], Kengo Nomura[1],

Sawako Tatsumi[1], Shinsuke Kido[1], Mikiko Ito[1,2], and Ken-ichi Miyamoto[1]

[1]*Department of Molecular Nutrition, Institution of Health Biosciences, the University of Tokushima Graduate School, Tokushima, Japan ; and [2]University of Hyogo School of Human Science and Environment, Hyogo, Japan*

Abstract : Mutations in the SLC34A3 gene, a sodium-dependent inorganic phosphate (Pi) cotransporter, also referred to as NaPi IIc, causes hereditary hypophosphatemic rickets with hypercalciuria (HHRH), an autosomal recessive disorder. In human and rodent, NaPi IIc is mainly localized in the apical membrane of renal proximal tubular cells. In this study, we identified mouse NaPi IIc variant (Npt2c-v1) that lacks the part of the exon 3 sequence that includes the assumed translation initiation site of Npt2c. Microinjection of mouse Npt2c-v1 cRNA into *Xenopus* oocytes demonstrated that Npt2c-v1 showed sodium-dependent Pi cotransport activity. The characterization of pH dependency showed activation at extracellular alkaline-pH. Furthermore, Npt2c-v1 mediated Pi transport activity was significantly higher at any pH value than those of Npt2c. In an in vitro study, the localization of the Npt2c-v1 protein was detected in the apical membrane in opossum kidney cells. The expression of Npt2c-v1 mRNA was detected in the heart, spleen, testis, uterus, placenta, femur, cerebellum, hippocampus, diencephalon and brain stem of mouse. Using mouse bone primary cultured cells, we showed the expression of Npt2c-v1 mRNA. In addition, the Npt2c protein was detected in the spermatozoa head. Thus, Npt2c-v1 was expressed in extra-renal tissues such as epididymal spermatozoa and may function as a sodium-dependent phosphate transporter. J. Med. Invest. 59 : 116-126, February, 2012

Keywords **:** *phosphate transporter, HHRH, Npt2c*

INTRODUCTION

Inorganic phosphate (Pi) reabsorption in the kidney proximal tubules is required for the survival of an organism. Sodium (Na)-dependent Pi transporters (NaPi) in the brush-border membrane of kidney proximal tubular cells mediate the rate-limiting step in the overall Pi reaborption process (1-9). The type IIa, type IIc and type III NaPi cotransporters (Slc34a1, SLC34A3 and SLC20A2 respectively) are expressed in the apical membrane of the proximal tubular cells and mediate Pi transport in kidney (1, 10, 11). Renal Pi reabsorption is regulated by dietary Pi intake, parathyroid hormone (PTH), fibroblast growth factor 23 (FGF23) and 1, 25-dihydroxyvitamin D (5, 8, 9, 11-16). In rodent, Pi reabsorption is

determined largely by the abundance of NaPi IIa (1, 8, 17, 18). NaPi IIc is more important in weaning animals than in adult animals, and its expression level is extremely low in adult kidney (1, 11, 15, 19, 20).

Hereditary hypophosphatemic rickets with hypercalciuria (HHRH) was identified recently (21-25). HHRH is a rare autosomal recessive inherited disorder that is characterized by hypophosphatemia, short stature, rickets and/or osteomalacia and secondary absorptive hypercalciuria (21-25). These reports indicated that NaPi IIc is important NaPi cotransporter in human kidney. However, in mouse, homozygous disrupted NaPi IIc gene causes markedly different biochemical features and the bone phenotype of HHRH (26). Thus, why mutations of the NaPi IIc gene cause HHRH, is still unknown. One possible explanation is that human NaPi IIc (NPT2c) has more profound roles in renal Pi reabsorption and bone mineralization than mouse NaPi IIc (Npt2c). The distribution of the NaPi IIc protein in mouse and human is still unknown. In the present study, we examined the distribution of Npt2c in various tissues and found a splice valiant of mouse Npt2c referred to here as Npt2c-v1. We have characterized the function and tissue distribution of Npt2c-v1 in mouse.

MATERIALS AND METHODS

Animals

Male C57BL/6 mice were purchased from the Charles River Laboratories Japan (Yokohama, Japan). The mice were housed in plastic cages and allowed free access to standard laboratory food and tap water. Animals were maintained under pathogen-free conditions and handled in accordance with the Guidelines for Animal Experimentation of Tokushima University School of Medicine, Japan.

cDNA cloning of Npt2c-v1

We obtained the cDNA clone for a mouse expressed sequence tag (EST) (GenBank™/EBI/ DDBJ accession no. AI956218) that we found by searching the EST data-base (dbEST) to show nucleotide sequence similarity to mouse Npt2c, was obtained from the Integrated and Molecular Analysis of Genomes and their Expression (IMAGE) resource. This mouse clone was sequenced in both directions using the dye terminator cycle sequencing method (Perkin-Elmer and Applied Biosystems).

The nucleotide sequence reported in this paper has been submitted to the GenBank™/EMBL Data Bank with accession number AB667978 which corresponding to Npt2c-v1 sequence.

Cell culture and transient transfection

Opossum kidney (OK) cells, kindly gifted by Drs. Heini Murer and Jung Biber (University of Zurich, Zurich, Switzerland), and MC3T3-E1 cells and COS-7 cells were cultured as described previously (27). The full-length mouse Npt2c and Npt2c-v1 genes were cloned into the plasmid pcDNA3.1(+) (Invitrogen, Carlsbad, CA). For transient transfection, cells were grown ~70% confluence, and 1 µg of cDNA were introduced with Lipofectamine according to the manufacturer's instructions (Invitrogen). After transfection, OK cells and COS-7 cells were used for immunostaining and immunoblotting respectively. For immunoblotting, the preparation of the membrane fraction was performed with Proteo Membrane Protein Extraction Kit (Calbiochem, San Diego, CA, USA). For immunostaining, OK cells were plated on glass coverslips in a 35 mm dish. After 48 h, cells were fixed with 3% paraformaldehyde and permeabilized with 0.1% Triton X-100/ PBS.

Isolated primary osteocytes and osteoblast from cortical bone

Primary osteocytes, and osteoblasts were isolated from mouse calvaria as described previously (28). Calvaria dissected from new born C57BL/6 mice, was dissolved in isolation buffer (25 mM HEPES, pH 7.4, 70 mM NaCl, 10 mM $NaHCO_3$, 60 mM sorbitol, 30 mM KCl, 3 mM K_2HPO_4, 1 mM $CaCl_2$, 1 mg/ml BSA, 5 mg/ml glucose, 5 mM EDTA) (28).

RNA extraction and RT-PCR

Total RNA were extracted from several mouse tissues using ISOGEN (Nippon gene, Tokyo, Japan), and cDNA was synthesized using the Moloney murine leukemia virus (M-MLV), Reverse transcriptase (Superscript, Invitrogen, Carlsbad, CA), and oligo(dT)12-18 primer. The PCR reactions were initiated with denaturation at $95°C$ for 10 min, followed by amplification with 40 cycles at $95°C$ for 30 s, annealing at $58°C$ for 30 s, and $72°C$ for 30 s.

PCR primer sequences were as follows : type IIc NaPi transporter (5'-CTCACCATACATGCA-G-3' and 5'-TGCCTAGTAGCTGGAAAGCA-3') ; GAPDH (5'-CTGCACCACCAACTGCTTAGC-3' and 5'-CATCCACAGTCTTCTGGGTG-3').

Xenopus oocyte expression and Pi transport analyses

cRNA obtained by *in vitro* transcription using T7 RNA polymerase for mouse Npt2c in plasmid vector pT7T3 were linearized with NotI (29). Npt2c-v1 was cloned into the plasmid vector pcDNA 3.1 (Invitrogen) and were linearized with XbaI and transcribed to cRNA with T7 polymerase. *Xenopus* oocyte expression studies and uptake measurements were performed as described previously (20). Briefly, *Xenopus* oocytes were surgically removed under sterile conditions from frogs anesthetized with 0.1% of 3-aminobenzoic acid ethyl ester (Sigma, St. Louis, MO). For expression studies, 25 ng cRNA coding for either mouse Npt2c or mouse Npt2c-v1 was injected into the oocytes. Four days after injection, measurements were carried out.

Pi transport analyses were examined as described previously (20). Group of six to eight oocytes were incubated in 500 μl of standard uptake solution ND100 (100 mM NaCl, 2 mM KCl, 1 mM $CaCl_2$, 1 mM $MgCl_2$, 10 mM HEPES/Tris, pH 7.5) containing 0.1 μCi. Sodium dependency of Pi (100 μM) transport was analyzed in ND100, Choline100 (100 mM Choline chloride, 2 mM KCl, 1 mM $CaCl_2$, 1 mM $MgCl_2$, 10 mM HEPES/Tris, pH 7.5) or Na gluconate100 (100 mM Na gluconate, 2 mM K gluconate, 1 mM Ca gluconate, 1 mM Mg gluconate, 10 mM HEPES/Tris, pH 7.5). Pi concentration dependence of Npt2c-v1 was measured at 3, 10, 30, 100, 300, and 1000 μM Pi in standard uptake solution and plotted against the Pi concentration. pH dependence of Npt2c-v1 mediated Pi (100 μM) uptake was measured in the standard uptake solution at various pH values (20).

Immunoblotting

Protein samples were heated at 95°C for 5 min in sample buffer in the presence of 2-mercaptoethanol and were subjected to SDS-polyacrylamide gel electrophoresis. The separated proteins were transferred by electrophoresis to Immobilon-P polyvinylidene difluoride membranes (Millipore, Billerica, MA) and then treated with diluted antibodies as follows : affinity purified anti Npt2c N-terminal (1 : 2500) or Npt2c C-terminal (1 : 1500) NaPi transporter antibodies. Mouse anti-actin monoclonal antibody (Chemicon, Temecula, CA) was used for internal control (16). Horseradish peroxidase-conjugated anti-rabbit or anti-mouse IgG was used as the secondary antibody (Jackson Immuno Research Laboratories, Inc, West Grove, PA), and signals were detected using the Immobilon™ Western Chemiluminescent HRP Substrate (Millipore).

Sperm collection

To collect epididymal sperm, epididymides were dissected from mice and immediately placed into cold PBS (140 mM NaCl, 10 mM phosphate buffer, pH 7.4) with protease inhibitor (PI) (Complete protease inhibitor cocktail, Roche Diagnostics, Mannheim, Germany). Epididymides were fragmented, and shake cultured at 37°C for 15 min. The suspension was centrifuged at $1200 \times g$ for 5 min at 4°C, and the pellet was suspended in PBS+PI. The pellet was centrifuged again and resuspended with PBS+PI (30).

Immunofluorescence analysis

Immunofluorescence analysis of mouse tissue sections was performed as described previously (16). Testis and epididymis were collected from mice, and soaked in 4% paraformaldehyde. Mice sperm were dried naturally on glass, and fixed with 4% paraformaldehyde, 0.25% glutaraldehyde in 0.1 M sodium phosphate buffer at pH 7.4 and acetone. For immunostaining, serial sections of mice tissue (5 μm), mice sperm or OK cells that were placed on the glass coverslips were incubated with affinity purified Npt2c N-terminal (1 : 100-1000) or C-terminal antibody (1 : 100-1000) over night at 4°C. Thereafter, sections were treated with Alexa Fluor 488 anti-rabbit IgG (Molecular Probes, Eugene, OR) (1 : 200) as a secondary antibody and Alexa Fluor 568-phalloidin (Molecular Probes) (1 : 200) to detect actin filaments for 60 min at room temperature.

Statistical Analysis

Data are expressed as means ± S.E. Statistical analysis was performed two-factor factorial ANOVA. $p < 0.05$ was considered to represent statistical significance.

RESULTS

Nucleotide sequence and predicted amino acid sequence of mouse Npt2c-v1

The Npt2c-v1 cDNA clone was 2,140 bp long with an open reading frame of 1,623 bp encoding 541 amino acid residues ; Npt2c has 601 amino acid residues. A comparison of the exon 3 nucleotide sequences of Npt2c and Npt2c-v1 is shown in Figure 1a. The Npt2c-v1 has 64 bp nucleotides that are

(a) Exon 3

```
Mouse Npt2c    5' CTAGGATTGGGCCTGGGTCTTCCCCTTCTTGAAATCCATGCCGAATTCCCTCGCCGGTGGCCAGGTCCCCAACCCTACTCTGGATGCCTTTGACCTGGTGGACCGGAGTCTGAGAAATGCAG-3'
Mouse Npt2c-v1 5' -----------------------------------------------------------------GTCCCCAACCCTACTCTGGATGCCTTTGACCTGGTGGACCGGAGTCTGAGAAATGCAG-3'
```

(b)
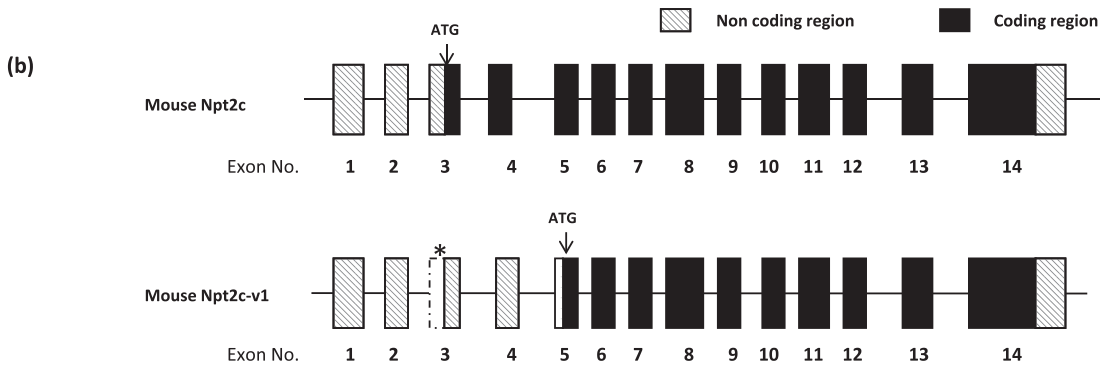
(c)

```
Mouse Npt2c      1  MPNSLAGGQVPNPTLDAFDLVDRSLRNAGISGSIPGLEEGGTDPWTFSPLKNADQLKEVGMASRLRRVVSSFLKACGLLGSLYFFICSLDILSSAFQLLG  100
Mouse Npt2c-v1   1  ----------------------------------------------------------MASRLRRVVSSFLKACGLLGSLYFFICSLDILSSAFQLLG   40

Mouse Npt2c    101  SKMAGDIFKDNVVLSNPVAGLVIGVLVTVLVQSSSTSSSIVVSMVASKLLTVQVSVPIIMGVNVGTSITSTLVSMAQSGDRDEFQRAFSGSAVHGIFNWL  200
Mouse Npt2c-v1  41  SKMAGDIFKDNVVLSNPVAGLVIGVLVTVLVQSSSTSSSIVVSMVASKLLTVQVSVPIIMGVNVGTSITSTLVSMAQSGDRDEFQRAFSGSAVHGIFNWL  140

Mouse Npt2c    201  TVLVLLPLESATAALERLSELALGAASLQPGQQAPDILKALTRPFTHLIIQLDSSVITSGITSNTTNSSLIKHWCGFRGETPQGSSEGCGLFSSCTERNS  300
Mouse Npt2c-v1 141  TVLVLLPLESATAALERLSELALGAASLQPGQQAPDILKALTRPFTHLIIQLDSSVITSGITSNTTNSSLIKHWCGFRGETPQGSSEGCGLFSSCTERNS  240

Mouse Npt2c    301  SASPEEDRLLCHHLFAGSKLTDLAVGFILLAGSLLVCVCLVLIVKLLNSVLRGRIAQAVRTVINADFPFPFGWLSGYLAILVGAGLTFLLQSSSVFTAA  400
Mouse Npt2c-v1 241  SASPEEDRLLCHHLFAGSKLTDLAVGFILLAGSLLVCVCLVLIVKLLNSVLRGRIAQAVRTVINADFPFPFGWLSGYLAILVGAGLTFLLQSSSVFTAA  340

Mouse Npt2c    401  IVPLMGVGVIDLERAYPLFLGSNIGTTTTALLAALASPADMLIFAVQVALIHFFFNLAGILLWYLVPVLRLPIPLAKRFGNLTAQYRWVAIVYLLLTFLL  500
Mouse Npt2c-v1 341  IVPLMGVGVIDLERAYPLFLGSNIGTTTTALLAALASPADMLIFAVQVALIHFFFNLAGILLWYLVPVLRLPIPLAKRFGNLTAQYRWVAIVYLLLTFLL  440

Mouse Npt2c    501  LPLAAFGLSLAGGTVLAAVGGPLVGLVLLIILVNVLQQHRPSWLPRCLQSWAWLPLWLHSLEPWDRLVTACCPCRACSNSPMTSKVAHCYENPQVIASQQ  600
Mouse Npt2c-v1 441  LPLAAFGLSLAGGTVLAAVGGPLVGLVLLIILVNVLQQHRPSWLPRCLQSWAWLPLWLHSLEPWDRLVTACCPCRACSNSPMTSKVAHCYENPQVIASQQ  540

Mouse Npt2c    601  L
Mouse Npt2c-v1 541  L
```
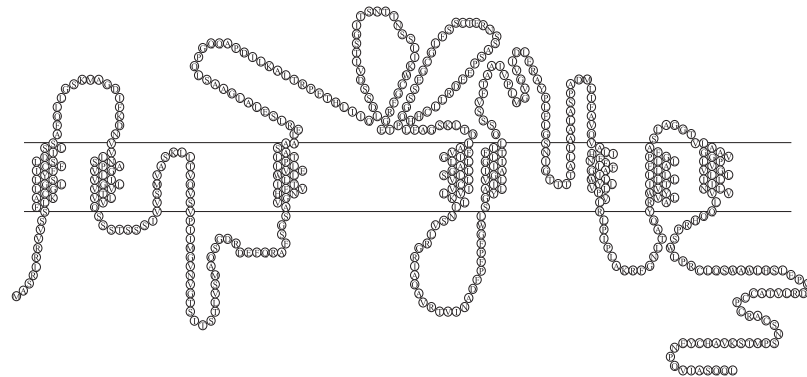
(d)
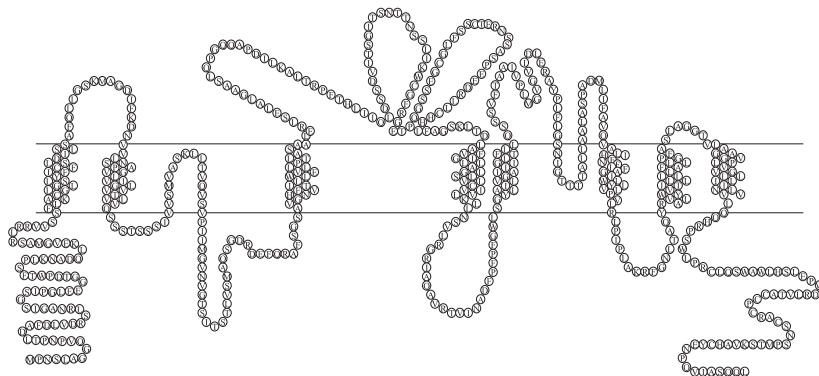
Figure 1.   Gene structure, nucleotides sequences and predicted amino acid sequences of mouse Npt2c and its splice valiant, Npt2c-v1
(a) Nucleotide sequences of exon3 of the genes. (b) Gene structure. *indicates the ablated region in exon 3 of the Npt2c-v1 mRNA.
(c) Predicted amino acid sequences of Npt2c and Npt2c-v1. (d) Predicted membrane topology of the Npt2c and Npt2c-v1 showing
the truncated region at the N-terminal of Npt2c-v1.

missing in exon 3 resulting in the deletion of the Npt2c translation start site. The predicted translation start site of Npt2c-v1 was located in exon 5 (Figure 1b) and the amino acid sequence translated from that site was completely consistent with the Npt2c amino acid sequence (Figure 1c). Hydropathy analysis of the presumed amino acid sequences of Npt2c and Npt2c-v1 revealed the presence of 12 putative transmembrane domains. In the topology model, the N-terminal intracellular loop of Npt2c is truncated by 50 amino acids in Npt2c-v1 (Figure 1d).

Western blotting and immunofluorescence analysis of Npt2c-v1

To assess the molecular weight of the Npt2c-v1 protein, western blotting analysis was performed (Figure 2). Npt2c and Npt2c-v1 were transfected into COS-7 cells. When the Npt2c N-terminal antibody was used to detect the presence of the proteins in the COS-7 membrane fraction, the Npt2c protein was seen at 63.9 kDa but the Npt2c-v1 protein was not detected (Figure 2-upper panel). In COS-7 cells membrane fraction, Npt2c was observed at 63.9 kDa and Npt2c-v1 was detected between 50 and 37 kDa using the Npt2c C-terminal antibody (Figure 2-lower panel). In the OK cells, similar observations were detected (data not shown).
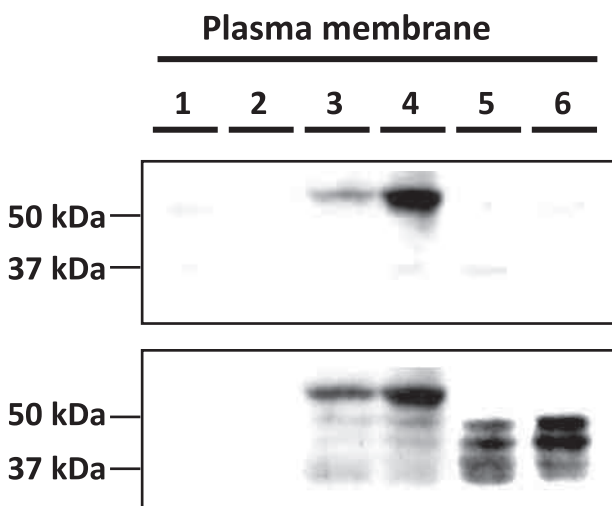
We also examined the localization of Npt2c and Npt2c-v1 in OK cells and *Xenopus* oocytes (Figure 3). In OK cells, Npt2c was observed in the apical membrane using both the Npt2c C-terminal and N-terminal antibodies (Figure 3a, b). Npt2c-v1 immunoreactive signals were detected in the apical membrane only with the Npt2c C-terminal antibody (Figure 3c) ; Npt2c-v1 was not observed when Npt2c N-terminal antibody was used (data not shown). Similarly, in *Xenopus* oocytes, the Npt2c and Npt2c-v1 proteins were localized in the plasma membrane (Figure 3d, e).
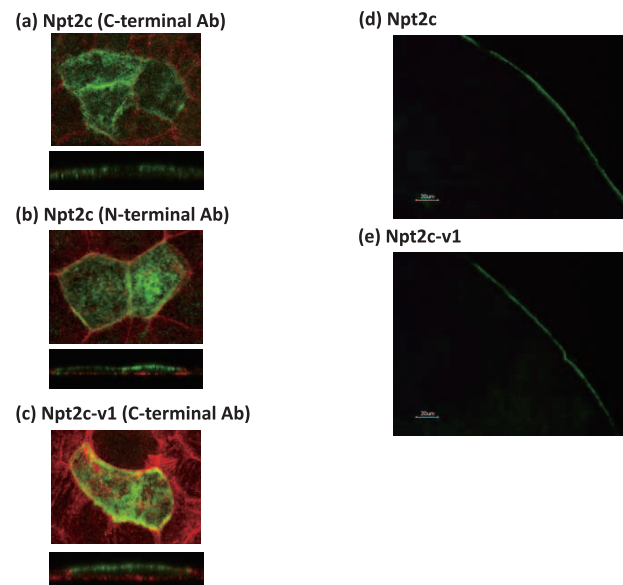

(a) Npt2c (C-terminal Ab)

(b) Npt2c (N-terminal Ab)

(c) Npt2c-v1 (C-terminal Ab)

(d) Npt2c

(e) Npt2c-v1

Figure 3.   Immunocytochemical analyses
Mouse Npt2c and Npt2c-v1 clones were transfected into OK cells (a-c), and cRNA were microinjected into *Xenopus* oocytes (d,e). (a, b) Npt2c. (c) Npt2c-v1. Expression of Npt2c (green) was detected using the Npt2c C-terminal antibody (a, c) and the Npt2c N-terminal antibody (b).
The expression of actin (red) was detected using phalloidin antibody (a-c).
The expression of Npt2c (d) and Npt2c-v1 (e) were detected using the Ntp2c C-terminal antibody.

Plasma membrane

| 1 | 2 | 3 | 4 | 5 | 6 |

50 kDa —
37 kDa —

50 kDa —
37 kDa —

Figure 2.   Expression analysis of Npt2c and Npt2c-v1 by molecular weight
Npt2c and Npt2c-v1 clones were transfected into COS-7 cells. Western blotting was performed in the plasma membrane in the presence of 2-mercaptoethanol. Only the Npt2c protein was detected by Npt2c N-terminal specific antibodies (upper panel). Both Npt2c and Npt2c-v1 proteins were detected by Npt2c C-terminal specific antibodies (lower panel). Lane 1, 2 ; Mock vector (pcDNA3.1). Lane 3, 4 ; Npt2c (pcDNA3.1). Lane 5, 6 ; Npt2c-v1 (pcDNA3.1).

The functional characteristics of Npt2c-v1 in Xenopus oocyte

Next, we analyzed the functional characteristics of Npt2c-v1 in *Xenopus* oocytes. As shown in Figure 4a, microinjection of Npt2c-v1 resulted in a marked increase in Pi transport activity, as well as in Npt2c activity. Npt2c-v1 mediated Pi transport activity was significantly higher than those of Npt2c (Figure 4a). Both Npt2c and Npt2c-v1 exhibited Pi transport activity that was dependent on Na^+ but not on Cl^- (Figure 4b). These results suggested that Npt2c-v1 is a NaPi transporter as well as Npt2c. The
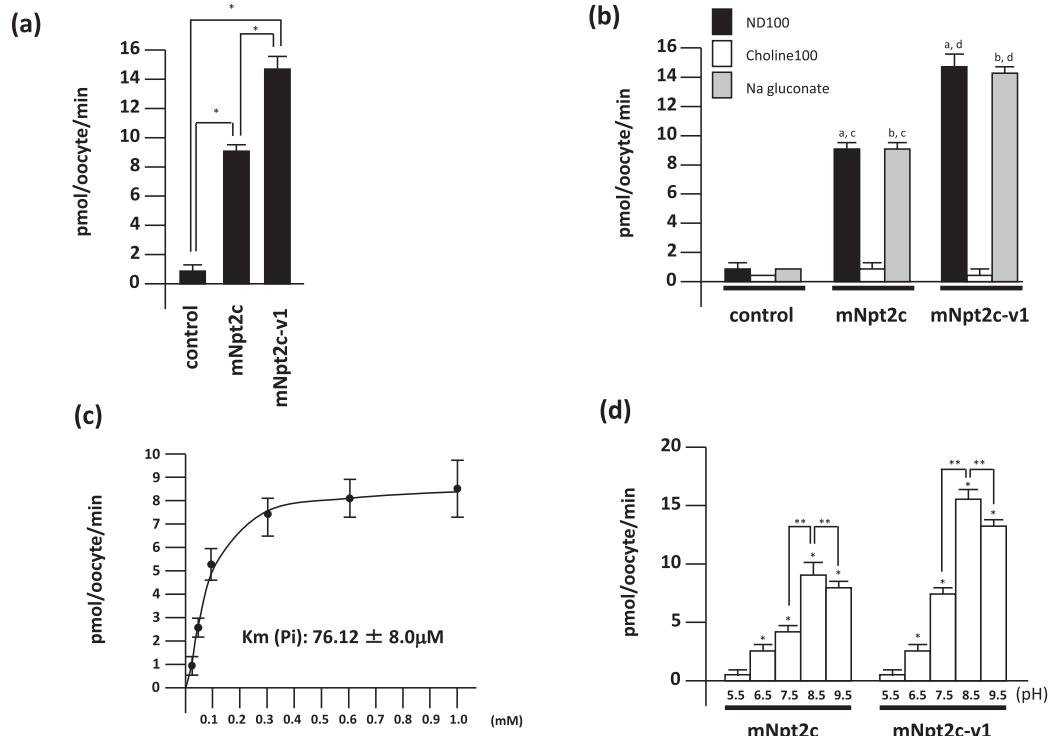
Figure 4.   Functional characterization of Npt2c-v1 in *Xenopus* oocytes
Pi transport activity in *Xenopus* oocytes was estimated using ^{32}P. (a) Pi transport was measured in ND100 at pH 7.5. * indicates $p <$ 0.05. (b) Sodium dependency of Pi transport was analyzed in ND100, Choline100, or Na gluconate buffer. a : $p < 0.05$ for water injected control in ND100, b : $p < 0.05$ for water injected control in Na gluconate, c : $p < 0.05$ for mNpt2c in Choline100, d : $p < 0.05$ for mNpt2c-v1 in Choline100. (c) Pi concentration dependence of Npt2c-v1 mediated Pi uptake. Pi uptake was measured at 3, 10, 30, 100, 300, and 1000 μM Pi in standard uptake solution (ND100 at pH 7.5) and plotted against the Pi concentration.
(d) pH-dependent phosphate transport assayed at pHs from 5.5 to 9.5. * indicates $p < 0.05$ at pH 5.5, ** indicates $p < 0.05$ at pH 8.5. Values are means ± SE ; n=6-10.

Michaelis-Menten constant (Km) for Pi was 76.12 ± 8.0 μM for Npt2c-v1 (Figure 4c). As shown in Figure 4d, Pi uptake mediated by Npt2c-v1 was enhanced at alkaline pH. We made two N-terminal truncated mutant clones del N24, and del N50. Using these clones, we characterized the functional properties of the N-terminal truncation mutants. The del N50 mutant clone also showed higher activity of Pi transport than Npt2c (data not shown).

Expression of Npt2c and Npt2c-v1 mRNA in various tissues

As described previously, Npt2c expression is highest in the kidney (29), and Npt2c mRNA is slightly expressed in several tissues (29). To determine whether Npt2c-v1 mRNA is expressed in those tissues of mouse, a set of PCR primers were designed to specifically synthesize the amplification of the Npt2c cDNAs and Npt2c-v1 cDNAs. Summarized in Table 1, Npt2c mRNA was detected in the kidney, spleen, testis, uterus, placenta, brain tissues and bone. Npt2c-v1 mRNA was observed in kidney, heart, testis, uterus, placenta, brain tissues and bone.

Table 1   Tissue distribution of Npt2c mRNA

	Npt2c	Npt2c-v1
kidney	+++	+
heart		+
spleen	+	
testis	+	+
uterus	+	+
placenta	+	+
brain tissues	+	+
calvaria	+	+
femur	+	+

Each tissues were obtained from wild type mice (n=3-6).

Thus, both Npt2c and Npt2c-v1 mRNA were identified in the kidney, testis, uterus placenta, brain tissues and bone, Npt2c mRNA was observed only in the spleen and Npt2c-v1 mRNA was observed only in the heart (Table 1). We also detected Npt2c and Npt2c-v1 mRNA expression in isolated osteoblasts and/or osteocytes from calvaria of newborn mice and in MC3T3-E1 cells (Figure 5).
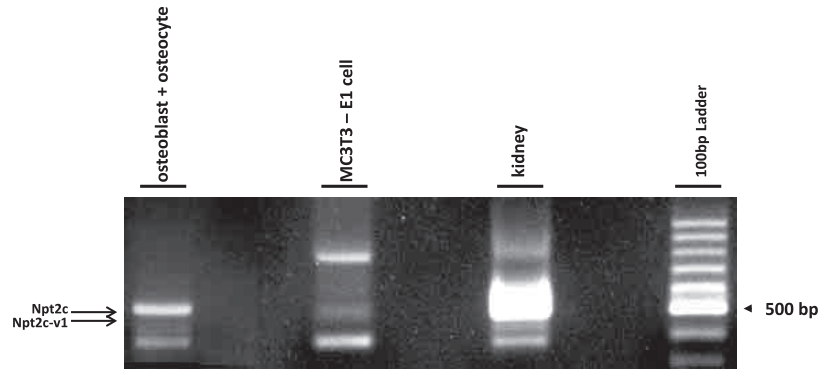
Figure 5.   Expression of Npt2c and Npt2c-v1 mRNA in bone cells
Primary cultured bone cells and MC3T3-E1 cells. RT-PCR was used to detect the Npt2c and Npt2c-v1. Both cells were examined at least twice (n=6).

Localization of Npt2c protein in testis, epididymis and spermatozoa

Using Npt2c specific antibodies, we examined the localization of Npt2c and Npt2c-v1 in bone tissue and in the primary cultured cells. In this study, our assay failed to detect positive signals in the bone tissue or in primary osteoblasts (data not shown).

When sections of mouse testis, epididymis and spermatozoa, were immunostained using Npt2c C-terminal antibody, we detected the staining of the Npt2c protein in spermatid and testicular spermatozoa (Figure 6). However the Npt2c protein was not detected in Sertoli cells, or in primary and secondary spermatocytes (Figure 6a-c). Thus, we focused our investigation on the localization of Npt2c-v1
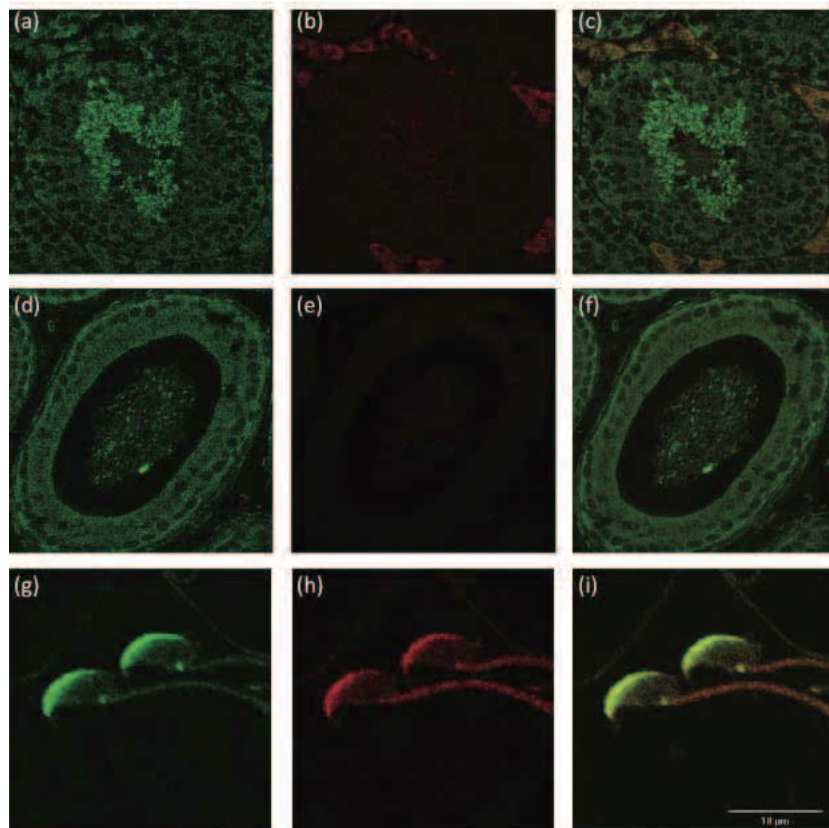

Figure 6.   Localization of Npt2c in mouse testis and epididymis by immunofluorescence staining
(a, b and c) Mouse testis, (d, e and f) epididymis and (g, h and i) spermatozoa from wild type mouse (n=3-6). Immunofluorescence staining of Npt2c was performed in paraffin-embedded of testis : (a, d) Npt2c (green) : (b, e) Actin (red) : (c, f) Marge. Magnification was x 1000. Npt2c was detected in mice spermatozoa using Npt2c C-terminal antibodies : (g) Npt2c (green), (h) Actin (red) ; and (i) Marge. Spermatozoa were collected from wild type mice (n=3-6).

in epididymis. The Npt2c-v1 protein was observed in the spermatozoa but not in the duct of the epididymis (Figure 6d-f). In the mouse spermatozoa, Npt2c-v1 was localized in the head of the spermatozoa, not in the flagellum region (Figure 6g-i).

DISCUSSION

In the present study, we identified and characterized a splice variant of Npt2c referred to as Npt2c-v1. Npt2c-v1 lacked the portion of the N-terminal region of the nucleotide sequence of exon 3 that included the putative translation start site of Npt2c. The predicted shortened amino acid sequence of Npt2c-v1 was assumed to be translated from the next in-frame start codon. If this is the correct start codon, then Npt2c-v1 encodes a protein of 541 amino acid residues that lacks 60 of the amino acid at the N-terminal end of Npt2c. Npt2c-v1 displayed most of the characteristics of Npt2c. Npt2c-v1 was localized in the plasma membrane and was shown to function as a sodium-dependent phosphate transporter with high affinity for Pi. The transport activity of Npt2c-v1 was dependent on the extracellular pH similar to Npt2c.

In this study, sodium-dependent Pi co-transport activity in Npt2c-v1 is higher than that of WT, suggesting that the N-terminal region may be involved in the NaPi cotransport activity. The current topological model of NaPi II family has been developed mainly using cysteine scanning and in vitro transcription/translation on NaPi IIa. The model comprises 12 transmembrane-spanning domains, intracellular located NH_2 and COOH terminal, and two N-glycosylation sites located in a large extracellular loop (31). An important structural feature of the NaPi II primary sequence is the two "repeat" regions in the NH_2- and COOH-terminal halves of the protein. These repeats are preserved in all NaPi IIa/b/c transporters as well as in homologs from *V. cholerae* and *C. elegans* (32), which strongly suggests that this conserved motif plays an essential functional role. Recent voltage clamp fluorometry (VCF) data also support the notion that the two halves of the NaPi IIb protein move in a complementary manner during the transport cycle (33). Although the role of N-terminal of NaPi IIc on Na^+-dependent Pi cotransport is not clear, VCF studies of Npt2c-v1 and WT may offer a view of molecular rearrangements that occur at specific sites during substrate interaction and translocation.

Mutations in the NPT2c/SLC34A3 gene cause HHRH (1, 21-24, 34) ; however, it is not clear why these mutations result in rickets. Npt2c knockout mice did not show rickets and/or osteomalacia-like phenotypes (1, 19, 26, 35). There are several possible explanations for these findings. One explanation was that the extra-renal expression of Npt2c might have an important role for phosphate homeostasis. In this study, we identified Npt2c-v1 expression in extra-renal tissues and characterized its function. Npt2c and Npt2c-v1 mRNAs were detected both in the primary osteocytes and osteoblasts from mouse cortical bone. Although the Npt2c and Npt2c-v1 mRNAs were detected in these primary cultured cells, we failed to detect expression of the Npt2c and Npt2c-v1 proteins. Indeed, Npt2c KO mice did not show any bone abnormality. More detailed studies are necessary to clarify the localization of Npt2c and its splice valiant in bone. Although we have not identified a human NPT2c-v1, several candidate of splice variants in rat and human NaPi IIc transcripts have detected (data not shown). Further studies are needed to clarify the roles of the human NPT2c splice variants.

In this study, we showed that the Npt2c-v1 transporter is expressed in sperm head. Spermatozoa, produced in the testis from spermatogonium and termed testicular spermatozoa, do not have fertilization ability (36-39). Motility and fertility are acquired during transit through the epididymis, and the maintenance of its circumstances is important for sperm maturation (36-39). Mammalian sperm has a head that contains the nucleus and acrosome, a midpiece with the mitochondria and the flagellum as the end piece (40). The importance of the flagellum in sperm motility is well known, and is regulated by the intracellular calcium concentration as a second messenger (40-44). The Pi transporters are thought to be localized in the plasma membrane (42, 45). How Pi concentration might affect spermatozoa motility and/or fertility is unknown. One possibility is that Pi is used as a constituent of phosphorylated molecules ; another is that as a Ca^{2+} influx regulatory factor, and Zarca *et al.* (42) have reported that extracellular Pi can influence Ca^{2+} transport. Furthermore, Xu *et al.* (46) have shown that the NaPi IIb has a potential role in male fertility. They reported that Pi concentration in epididymis luminal fluid might influence sperm fertility. It have been suggested that the over expression of NaPi IIb results in low Pi concentration in cauda luminal fluid leading to inadequate maturation of spermatozoa

(46). These results strongly imply that Pi is crucial for maturation of spermatozoa and fertility.

Upon ejaculation spermatozoa are exposed to higher extracellular pH making them motile for the first time (47-50). During subsequent transit through the female reproduction tract, the intracellular pH of the sperm further increases as the result of sperm capacitation (47). If Npt2c/Npt2c-v1 is activated at alkaline pH, this would be convenient for the sperm in terms of ATP production by Pi influx. Based on these results, we suggest that Npt2c/Npt2c-v1 is a candidate of NaPi transporter in sperm.

Finally, in the present study, we identified a splice valiant of Npt2c and studied its functional characterization. Npt2c-v1 was identified as a sodium-dependent phosphate transporter. The presence of Npt2c and/or Npt2c-v1 was detected in several mouse tissues, including bone and sperm head. Further studies are needed to clarify the role of Npt2c-v1 in extra-renal tissues.

Financial Support

CONFLICT OF INTEREST

None of the authors have any conflicts of interest to declare.

REFERENCES

1. Segawa H, Aranami F, Kaneko I, Tomoe Y, and Miyamoto K : The roles of Na/Pi-II transporters in phosphate metabolism. Bone 45 (Suppl 1) : S2-7, 2009
2. Murer H, Hernando N, Forster I, and Biber J : Proximal tubular phosphate reabsorption : molecular mechanisms. Physiol Rev 80 : 1373-1409, 2000
3. Tenenhouse HS, and Sabbagh Y : Novel phosphate-regulating genes in the pathogenesis of renal phosphate wasting disorders. Pflügers Arch 444 : 317-326, 2002
4. Yu X, and White KE : FGF23 and disorders of phosphate homeostasis. Cytokine Growth Factor Rev 16 : 221-232, 2005
5. Segawa H, Kawakami E, Kaneko I, Kuwahata M, Ito M, Kusano K, Saito H, Fukushima N, and Miyamoto K : Effect of hydrolysis-resistant FGF23-R179Q on dietary phosphate regulation of the renal type-II Na/Pi transporter. Pflügers Arch 446 : 585-592, 2003
6. Inoue Y, Segawa H, Kaneko I, Yamanaka S, Kusano K, Kawakami E, Furutani J, Ito M, Kuwahata M, Saito H, Fukushima N, Kato S, Kanayama HO, and Miyamoto K : Role of the vitamin D receptor in FGF23 action on phosphate metabolism. Biochem J 390 : 325-331, 2005
7. Miyamoto K, Ito M, Kuwahata M, Kato S, and Segawa H : Inhibition of intestinal sodium-dependent inorganic phosphate transport by fibroblast growth factor 23. Ther Apher Dial 9 : 331-335, 2005
8. Miyamoto K, Segawa H, Ito M, and Kuwahata M : Physiological regulation of renal sodium-dependent phosphate cotransporters. Jpn J Physiol 54 : 93-102, 2004
9. Berndt T, and Kumar R : Novel mechanisms in the regulation of phosphorus homeostasis. Physiology (Bethesda) 24 : 17-25, 2009
10. Murer H, Forster I, and Biber J : The sodium phosphate cotransporter family SLC34. Pflügers Arch 447 : 763-767, 2004
11. Tenenhouse HS : Regulation of phosphorus homeostasis by the type iia na/phosphate cotransporter. Annu Rev Nutr 25 : 197-214, 2005
12. Segawa H, Yamanaka S, Ito M, Kuwahata M, Shono M, Yamamoto T, and Miyamoto K : Internalization of renal type IIc Na-Pi cotransporter in response to a high-phosphate diet. Am J Physiol Renal Physiol 288 : F587-596, 2005
13. Tomoe Y, Segawa H, Shiozawa K, Kaneko I, Tominaga R, Hanabusa E, Aranami F, Furutani J, Kuwahara S, Tatsumi S, Matsumoto M, Ito M, and Miyamoto K : Phosphaturic action of fibroblast growth factor 23 in Npt2 null mice. Am J Physiol Renal Physiol 298 : F1341-1350, 2010
14. Murer H, Lotscher M, Kaissling B, Levi M, Kempson SA, and Biber J : Renal brush border membrane Na/Pi-cotransport : molecular aspects in PTH-dependent and dietary regulation. Kidney Int 49 : 1769-1773, 1996
15. Kaneko I, Segawa H, Furutani J, Kuwahara S, Aranami F, Hanabusa E, Tominaga R, Giral H, Caldas Y, Levi M, Kato S, and Miyamoto K :

Hypophosphatemia in vitamin D receptor null mice : effect of rescue diet on the developmental changes in renal Na+ -dependent phosphate cotransporters. Pflügers Arch 461 : 77-90, 2011

16. Segawa H, Yamanaka S, Onitsuka A, Tomoe Y, Kuwahata M, Ito M, Taketani Y, and Miyamoto K : Parathyroid hormone-dependent endocytosis of renal type IIc Na-Pi cotransporter. Am J Physiol Renal Physiol 292 : F395-403, 2007

17. Biber J, Hernando N, Forster I, and Murer H : Regulation of phosphate transport in proximal tubules. Pflügers Arch 458 : 39-52, 2009

18. Miyamoto K, Ito M, Tatsumi S, Kuwahata M, and Segawa H : New aspect of renal phosphate reabsorption : the type IIc sodium-dependent phosphate transporter. Am J Nephrol 27 : 503-515, 2007

19. Miyamoto K, Haito-Sugino S, Kuwahara S, Ohi A, Nomura K, Ito M, Kuwahata M, Kido S, Tatsumi S, Kaneko I, and Segawa H : Sodium-dependent phosphate cotransporters : lessons from gene knockout and mutation studies. J Pharm Sci 100 : 3719-3730, 2011

20. Segawa H, Kaneko I, Takahashi A, Kuwahata M, Ito M, Ohkido I, Tatsumi S, and Miyamoto K : Growth-related renal type II Na/Pi cotransporter. J Biol Chem 277 : 19665-19672, 2002

21. Bergwitz C, Roslin NM, Tieder M, Loredo-Osti JC, Bastepe M, Abu-Zahra H, Frappier D, Burkett K, Carpenter TO, Anderson D, Garabedian M, Sermet I, Fujiwara TM, Morgan K, Tenenhouse HS, and Juppner H : SLC34A3 mutations in patients with hereditary hypophosphatemic rickets with hypercalciuria predict a key role for the sodium-phosphate cotransporter NaPi-IIc in maintaining phosphate homeostasis. Am J Hum Genet 78 : 179-192, 2006

22. Lorenz-Depiereux B, Benet-Pages A, Eckstein G, Tenenbaum-Rakover Y, Wagenstaller J, Tiosano D, Gershoni-Baruch R, Albers N, Lichtner P, Schnabel D, Hochberg Z, and Strom TM : Hereditary hypophosphatemic rickets with hypercalciuria is caused by mutations in the sodium-phosphate cotransporter gene SLC34A3. Am J Hum Genet 78 : 193-201, 2006

23. Ichikawa S, Sorenson AH, Imel EA, Friedman NE, Gertner JM, and Econs MJ : Intronic deletions in the SLC34A3 gene cause hereditary hypophosphatemic rickets with hypercalciuria. J Clin Endocrinol Metab 91 : 4022-4027, 2006

24. Yamamoto T, Michigami T, Aranami F, Segawa H, Yoh K, Nakajima S, Miyamoto K, and Ozono K : Hereditary hypophosphatemic rickets with hypercalciuria : a study for the phosphate transporter gene type IIc and osteoblastic function. J Bone Miner Metab 25 : 407-413, 2007

25. Beck L, Karaplis AC, Amizuka N, Hewson AS, Ozawa H, and Tenenhouse HS : Targeted inactivation of Npt2 in mice leads to severe renal phosphate wasting, hypercalciuria, and skeletal abnormalities. Proc Natl Acad Sci USA 95 : 5372-5377, 1998

26. Segawa H, Onitsuka A, Kuwahata M, Hanabusa E, Furutani J, Kaneko I, Tomoe Y, Aranami F, Matsumoto N, Ito M, Matsumoto M, Li M, Amizuka N, and Miyamoto K : Type IIc sodium-dependent phosphate transporter regulates calcium metabolism. J Am Soc Nephrol 20 : 104-113, 2009

27. Ito M, Iidawa S, Izuka M, Haito S, Segawa H, Kuwahata M, Ohkido I, Ohno H, and Miyamoto K : Interaction of a farnesylated protein with renal type IIa Na/Pi co-transporter in response to parathyroid hormone and dietary phosphate. Biochem J 377 : 607-616, 2004

28. Gu G, Nars M, Hentunen TA, Metsikko K, and Väänänen HK : Isolated primary osteocytes express functional gap junctions in vitro. Cell Tissue Res 323 : 263-271, 2006

29. Ohkido I, Segawa H, Yanagida R, Nakamura M, and Miyamoto K : Cloning, gene structure and dietary regulation of the type-IIc Na/Pi cotransporter in the mouse kidney. Pflügers Arch 446 : 106-115, 2003

30. Wang D, King SM, Quill TA, Doolittle LK, and Garbers DL : A new sperm-specific Na+/H+ exchanger required for sperm motility and fertility. Nat Cell Biol 5 : 1117-1122, 2003

31. Forster IC, Hernando N, Biber J, and Murer H : Proximal tubular handling of phosphate : A molecular perspective. Kidney Int 70 : 1548-1559, 2006

32. Werner A, and Kinne RK : Evolution of the Na-P(i) cotransport systems. Am J Physiol Regul Integr Comp Physiol 280 : R301-312, 2001

33. Virkki LV, Murer H, and Forster IC : Voltage clamp fluorometric measurements on a type II Na+-coupled Pi cotransporter : shedding light on substrate binding order. J Gen Physiol 127 : 539-555, 2006

34. Jaureguiberry G, Carpenter TO, Forman S, Juppner H, and Bergwitz C : A novel missense

mutation in SLC34A3 that causes hereditary hypophosphatemic rickets with hypercalciuria in humans identifies threonine 137 as an important determinant of sodium-phosphate cotransport in NaPi-IIc. Am J Physiol Renal Physiol 295 : F371-379, 2008

35. Segawa H, Onitsuka A, Furutani J, Kaneko I, Aranami F, Matsumoto N, Tomoe Y, Kuwahata M, Ito M, Matsumoto M, Li M, Amizuka N, and Miyamoto K : Npt2a and Npt2c in mice play distinct and synergistic roles in inorganic phosphate metabolism and skeletal development. Am J Physiol Renal Physiol 297 : F671-678, 2009

36. Sonnenberg-Riethmacher E, Walter B, Riethmacher D, Godecke S, and Birchmeier C : The c-ros tyrosine kinase receptor controls regionalization and differentiation of epithelial cells in the epididymis. Genes Dev 10 : 1184-1193, 1996

37. Yeung CH, Wagenfeld A, Nieschlag E, and Cooper TG : The cause of infertility of male c-ros tyrosine kinase receptor knockout mice. Biol Reprod 63 : 612-618, 2000

38. Yeung CH, Sonnenberg-Riethmacher E, and Cooper TG : Infertile spermatozoa of c-ros tyrosine kinase receptor knockout mice show flagellar angulation and maturational defects in cell volume regulatory mechanisms. Biol Reprod 61 : 1062-1069, 1999

39. Yeung CH, Sonnenberg-Riethmacher E, and Cooper TG : Receptor tyrosine kinase c-ros knockout mice as a model for the study of epididymal regulation of sperm function. J Reprod Fertil (Suppl 53) : 137-147, 1998

40. Publicover S, Harper CV, and Barratt C : [Ca2+]i signalling in sperm--making the most of what you've got. Nat Cell Biol 9 : 235-242, 2007

41. Darszon A, Acevedo JJ, Galindo BE, Hernandez-Gonzalez EO, Nishigaki T, Trevino CL, Wood C, and Beltran C : Sperm channel diversity and functional multiplicity. Reproduction 131 : 977-988, 2006

42. Zarca A, Rubinstein S, and Breitbart H : Transport mechanism for calcium and phosphate in ram spermatozoa. Biochim Biophys Acta 944 : 351-358, 1988

43. Baker MA, Hetherington L, Ecroyd H, Roman SD, and Aitken RJ : Analysis of the mechanism by which calcium negatively regulates the tyrosine phosphorylation cascade associated with sperm capacitation. J Cell Sci 117 : 211-222, 2004

44. Jimenez-Gonzalez C, Michelangeli F, Harper CV, Barratt CL, and Publicover SJ : Calcium signalling in human spermatozoa : a specialized 'toolkit' of channels, transporters and stores. Hum Reprod Update 12 : 253-267, 2006

45. Babcock DF, First NL, and Lardy HA : Transport mechanism for succinate and phosphate localized in the plasma membrane of bovine spermatozoa. J Biol Chem 250 : 6488-6495, 1975

46. Xu Y, Yeung CH, Setiawan I, Avram C, Biber J, Wagenfeld A, Lang F, and Cooper TG : Sodium-inorganic phosphate cotransporter NaPi-IIb in the epididymis and its potential role in male fertility studied in a transgenic mouse model. Biol Reprod 69 : 1135-1141, 2003

47. Suarez SS : Control of hyperactivation in sperm. Hum Reprod Update 14 : 647-657, 2008

48. Ho HC, Granish KA, and Suarez SS : Hyperactivated motility of bull sperm is triggered at the axoneme by Ca2+ and not cAMP. Dev Biol 250 : 208-217, 2002

49. Axner E : Sperm maturation in the domestic cat. Theriogenology 66 : 14-24, 2006

50. Maas DH, Storey BT, and Mastroianni L, Jr. : Hydrogen ion and carbon dioxide content of the oviductal fluid of the rhesus monkey (Macaca mulatta). Fertil Steril 28 : 981-985, 1977